Topology Optimization of Quasi-periodic Cellular Structures Using a Hybrid MMC-Density Approach

Pengfei Xiao , Chunping Zhou , Yongxin Qu , Yunfeng Luo * , Quhao Li *

Posted Date: 11 July 2024

doi: 10.20944/preprints202407.0902.v1

Keywords: topology optimization; quasi-periodic cellular structure; moving morphable components method; asymptotic homogenization method

Article

Topology Optimization of Quasi-Periodic Cellular Structures Using a Hybrid MMC-Density Approach

Pengfei Xiao [1], Chunping Zhou [2], Yongxin Qu [3], Yunfeng Luo [2,*] and Quhao Li [2,*]

[1] AVIC Research Institute for Special Structures of Aeronautical Composites, Jinan, Shandong Province, 210000, China, China; 13163339094@163.com (P.X.);
[2] Key Laboratory of High Efficiency and Clean Mechanical Manufacture of MOE, School of Mechanical Engineering, Shandong University, Jinan 250061, China; 3378099369@qq.com
* Correspondence: luoyunfeng@sdu.edu.cn (Y.L.); quhaoli@sdu.edu.cn (Q.L.)

Abstract: Porous hierarchical structure has been widely used in engineering for its high specific strength and stiffness, improved corrosion-resistance and multifunctionality. The design of multi-scale topology optimization for such structures has been a hot topic during the past two decades. In this paper, a new hybrid MMC-density topology optimization method of cellular structures with quasi-periodic microstructures is proposed. The so-called 'quasi-periodic' means the microstructures in different macro points have similar topology but with different parameters. The key idea is to describe the microstructural topology using MMC and describe the micro layout using the variable density. Sensitivities of the structural compliance with respect to the two types of design variables are derived and gradient optimization method is applied to update the design variables. The presented numerical examples show that the quasi-periodic cellular structures have better performance than single-scale structures and periodic cellular structures. Numerical examples demonstrate the effectiveness of the proposed approach.

Keywords: topology optimization; quasi-periodic cellular structure; moving morphable components method; asymptotic homogenization method

1. Introduction

Cellular structures are widely existing in natural biological structures (e.g. plant stems or animal bones), and have attracted great attention for their superior structural performances. Lots of biomimetic cellular structures are witnessed in many industry fields like aerospace, automobile, biomedical, etc. [1]. In recent years, with the rapid development of advanced manufacturing technologies, especially additive manufacturing, cellular structures with more complex geometry [2–4] can be fabricated. Thus, how to systematic design cellular structures for satisfying the specific engineering demands, is a hot topic in design area.

Topology optimization is an automatic design method which can provide new and even unanticipated design ideas by finding the optimum material layout for prescribed design objective and constraints. It has been successfully applied in many engineering structures [5,6]. Besides, by combining the topology optimization method with homogenization method, a large number of architected materials with desired elastic, thermal, and fluidic properties were obtained [7–10]. Interested readers can refer to the literatures [11–14] for comprehensive reviews.

Compared to the single-scale structures, cellular structures have two or more coupled scales and this brings the difficulties to the topology optimization problem. One simple but computational-cost method is to discrete the design domain with fine mesh covering both macro and micro scales. Then the same procedure as the single-scale topology optimization can be used [15]. However, this method generally requires a mass of mesh which results a large amount of computation.

The other method is to use the multiscale finite element method [16] or homogenization method [17,18] to separate the two scales for reduce the amount of computation. The representative works can refer to the researches by Rodrigues et al. [19] and Xia et al. [20,21] . In their works, the macro-

 doi:10.20944/preprints202407.0902.v1

scale material distribution as well as the corresponding local microstructures were optimized simultaneously. These optimized results have point-varied microstructures and show good structural performances. But since inverse-homogenization are required for all macro elements, these methods still need large computational cost and the optimized results lack of the connectivity between the neighboring microstructures. Besides, the optimization models and the solving processes are too complicated in multi-physics or multi-constrained problems [22]. For solve these problems, Yan and Cheng et al. [23,24] proposed a concurrent method to design the periodic cellular structures. This method has a simple topology optimization formulation and needs only small computational cost. So, it was extended to various types of topology optimization problems, e.g. the thermal-elastic problems [25–27], the dynamic problems [28–30], the uncertain problems [31,32], and the multi-functionality optimization problems [33]. However, since this type of structure has an identical microstructure, the material properties cannot vary within the macro-domain. This restricts the structural performance improvement.

Quasi-periodic cellular structure is a special type of multi-scale structures. The 'quasi-periodic' means the microstructures share the similar topology while one or more parameters in the microstructures, can be varied. In this paper, these parameters are named as *alterable parameters*. By optimizing these alterable parameters, microstructures can have different densities and mechanical properties in different macro points, thus quasi-periodic cellular structures have larger design space than periodic cellular structures. Besides, the neighboring microstructures are connectable naturally since they share the similar microstructural topology. Zhang et.al. [34] chosen the radii of the circular holes in the cellular as the design variables and a nearly 35% stiffness increment was obtained compared to the uniform hexagonal cellular structure. Similarly, a nearly 40% natural frequency enhancement can be seen by optimizing the sizes of the hexagonal holes in the square microstructures [35]. Cheng et.al [36] introduced an anisotropic yield criterion of the lattice structure for the design of the quasi-periodic cellular structures with stress constraints. Wu et.al [37] proposed an approximation of reduced substructure with penalization model to optimize the quasi-periodic lattice structures for considering the scaling effects. Nevertheless, the microstructural topology used in these works are prescribed and not optimized.

Wang et al. [38,39] proposed to describe a family of quasi-periodic microstructures by cutting the signed distance function in different locations. Then, both the spatially varying microstructural topology and their macroscopic distribution are optimized in a sequential processing. On this basis, Zong et.al. [40] presents a variable cutting function by interpolating with a set of height variables located in nodes for guaranteeing the perfect geometric connections between adjacent cells. By these ways, concurrent optimization of the microstructural topology and the distribution of alterable parameters was realized in level-set topology optimization framework.

Recently, Guo et al. [41–43] proposed a novel topology optimization approach based on the concept of MMC. Unlike traditional topology optimization methods using element/node variables, the methods using the geometric parameters of the components as design variables. Since the MMC method uses the explicit parameters to describe a component, so it is convenient to define an alterable parameter. Therefore, the number of design variables can be reduced considerably. Furthermore, using the geometric parameters to describe the geometries of the components allows us to establish a direct link with computer-aided-design systems. Then, the topology of the base unit cell and the distribution of these quasi-periodic microstructures in macro scale are optimized simultaneously. Compliance minimum problem with volume constraint is considered in this paper and the method of Moving Asymptotes (MMA) [44] is used to solve the optimization models based on the derived sensitivity formulations.

The organization of the rest of this paper is as follows. The new topological description method of the quasi-periodic structures is given in Section 2. Then Section 3 presents the optimization model formulation and deals with the structural sensitivity analysis required for numerical optimization algorithms. An optimization procedure in terms of the pseudo code is presented in Section 4. Section 5 outlines three numerical examples to validate the effectiveness of the proposed method. Finally, a conclusion closes the paper.

Preprints.org (www.preprints.org) | NOT PEER-REVIEWED | Posted: 11 July 2024 doi:10.20944/preprints202407.0902.v1

2. Problem Formulation

This section presents a new topological description method of quasi-periodic cellular structures in the MMC framework. Firstly, a brief description of the MMC method is given for render the paper self-contained. Then, the design variables used to describe the quasi-periodic cellular structures are defined. Topology optimization formulation is listed in the end.

2.1. Moving Morphable Component (MMC) Method

Differ from conventional density-based framework or level-set method, the moving morphable component (MMC) approach uses a series of structural components to describe a structural topology. It defines that the region occupied by structural components is filled with solid material and the others are void, which means:

$$\phi^s(\mathbf{x})\begin{cases} >0, & if \ \ \mathbf{x}\in\Omega^s, \\ =0, & if \ \ \mathbf{x}\in\partial\Omega^s, \\ <0, & if \ \ \mathbf{x}\in D\setminus\Omega^s. \end{cases} \tag{1}$$

where D represents a design domain and $\Omega^s \subset D$ denotes a subset of D occupied by components. Here, $\phi^s(\mathbf{x})$ can be computed by:

$$\phi^s(\mathbf{x}) = \max(\phi_1,...,\phi_n) \tag{2}$$

where $\phi_i = \phi_i(\mathbf{x}), i = 1,...n$ denoting the topology description function (TDF) of the region occupied by the i-th component (i.e. Ω_i,), as shown in Figure 1.

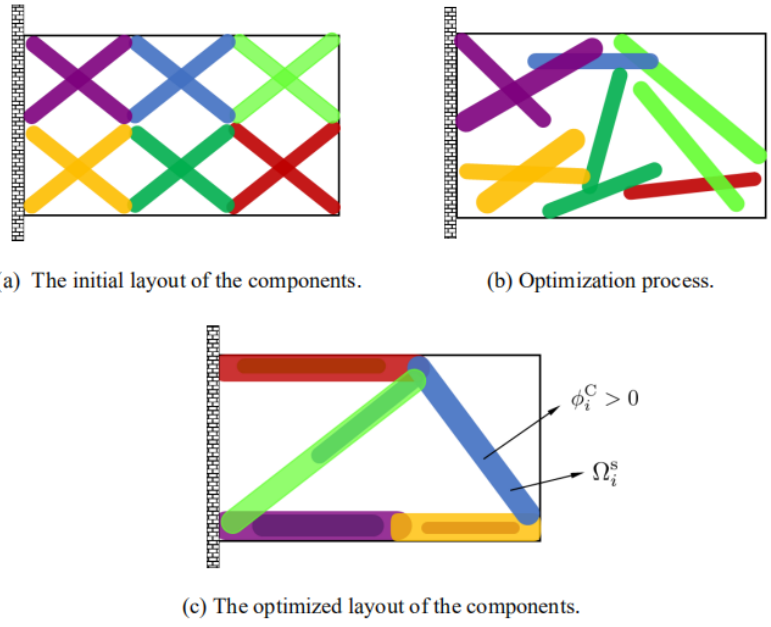

Figure 1. The representation of structural topology through the level set functions of each component.

Many functions have been used to describe the components, such as Super-ellipses, Closed B-Splines (CBS) and so on [43,45,46]. In the present paper, the following TDF proposed by Guo etc. [47] is used owing to its simplicity:

 doi:10.20944/preprints202407.0902.v1

$$\phi_i(x,y)=\left(\frac{x'}{L_i}\right)^p+\left(\frac{y'}{f(x')}\right)^p-1 \tag{3}$$

with

$$\begin{Bmatrix} x' \\ y' \end{Bmatrix}=\begin{bmatrix} \cos\theta_i & \sin\theta_i \\ -\sin\theta_i & -\cos\theta_i \end{bmatrix}\begin{Bmatrix} x-x_{0i} \\ y-y_{0i} \end{Bmatrix} \tag{4}$$

where $f(x')$ is a function depicts the shapes of the components along the x' direction. p is a relatively large integer number (p=6 is used in the present study), (x_{0i}, y_{0i}) denotes the coordinate of the center of the component, L_i denotes the half length of the component and θ_i is the inclined angle of the component. By using these parameters, the boundary and geometry features of a component can be described explicitly. In this paper, the quadratically varying thicknesses function is used (as shown in Figure 2):

$$f(x')=\frac{t^1+t^2-2t^3}{2L^2}(x')^2+\frac{t^2-t^1}{2L}x'+t^3 \tag{5}$$

where t^1, t^2 and t^3 denote the thickness of a component, L is the length of a component.

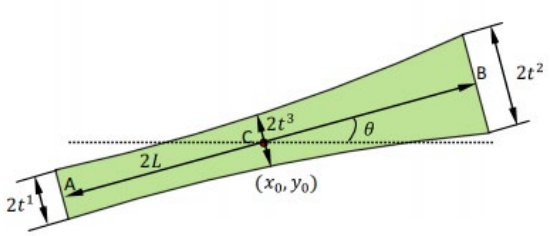

Figure 2. Geometry description of a structural component.

2.2. Topological Description of Quasi-Periodic Cellular Structures

To describe a quasi-periodic cellular structure, two procedures are contained. One is describing the topology of the base unit cell (BUC), and the other one is choosing an alterable parameter to obtain a family of quasi-microstructures from a BUC. As shown in last section, the MMC method has explicit parameters to describe the components, which gives a more convenient way to define the alterable parameter than other methods. Thus, the MMC method is applied to describe the topology of the BUC in this work. The topology of the BUC can be determined by a design vector $\mathbf{D}^{mi}$:

$$\mathbf{D}^{mi}=\left(\left(\mathbf{D}^1\right)^{\mathrm{T}},\ldots,\left(\mathbf{D}^i\right)^{\mathrm{T}},\ldots\left(\mathbf{D}^{N^{mi}}\right)^{\mathrm{T}}\right)^{\mathrm{T}} \tag{6}$$

where $\mathbf{D}^i=\left(x_{0i},y_{0i},L_i,\theta_i,\mathrm{t}_i^1,\mathrm{t}_i^2,\mathrm{t}_i^3\right)^{\mathrm{T}}$ is the parameter vector of the i-th component, N^{mi} is the number of components. In order to get a series of quasi-periodic microstructures with a simple alterable parameter from the BUC, we define a parameter R which can scale the thickness of all components in the base unit cell, as shown in Figure 3, this means:

$$\left[\mathrm{t}_i^1,\mathrm{t}_i^2,\mathrm{t}_i^3\right]_Q=R*\left[\mathrm{t}_i^1,\mathrm{t}_i^2,\mathrm{t}_i^3\right]_B \tag{7}$$

where subscript Q and B represents the quasi-periodic microstructures and base unit cell (BUC), respectively. Obviously, R<1 means the thickness of the components will be thinned and the

Preprints.org (www.preprints.org) | NOT PEER-REVIEWED | Posted: 11 July 2024 doi:10.20944/preprints202407.0902.v1

microstructures with smaller volume fraction can be obtained. While for R>1, the thickness of the components will be thickened and this results some microstructures with larger volume fraction. If we increase the R form a small value (for example 0.1) with small steps until the cell is full filled solid materials, we can obtain a family of quasi-periodic microstructures. The volume fraction of each quasi-periodic microstructures can be computed by:

$$V_{mi} = \frac{\int_D H\left(\phi^s\left(\mathbf{x}\right)\right)dV}{V} \tag{8}$$

where D denotes the micro domain and V represents the volume of the micro domain. H=H(x) is the Heaviside function:

$$H\left(x\right) = \begin{cases} 1 & x \geq 0 \\ 0 & x < 0 \end{cases} \tag{9}$$

After obtain a family of quasi-periodic microstructures, the next step is determine the optimal distribution of these microstructures in the macro-domain. The most direct way is to set the vector $\mathbf{R}_{ma}$ as the design variables. Thus by optimizing the R for desired objective and constraint functions, the optimal quasi-periodic cellular structure can be obtained. But unfortunately, in this way, the bounds of R are difficult to be determined. For solving this problem, element density $0 \leq \boldsymbol{\rho}^{ma} \leq 1$ is defined as design variable instead of R in the macro design. ρ_e^{ma}=0 and ρ_e^{ma}=1 represent the void and solid, respectively. For $0 < \rho_e^{ma} < 1$, the corresponding microstructure with the same volume fraction is placed in the macro domain. Here, subscript e represents the index of the design variable.

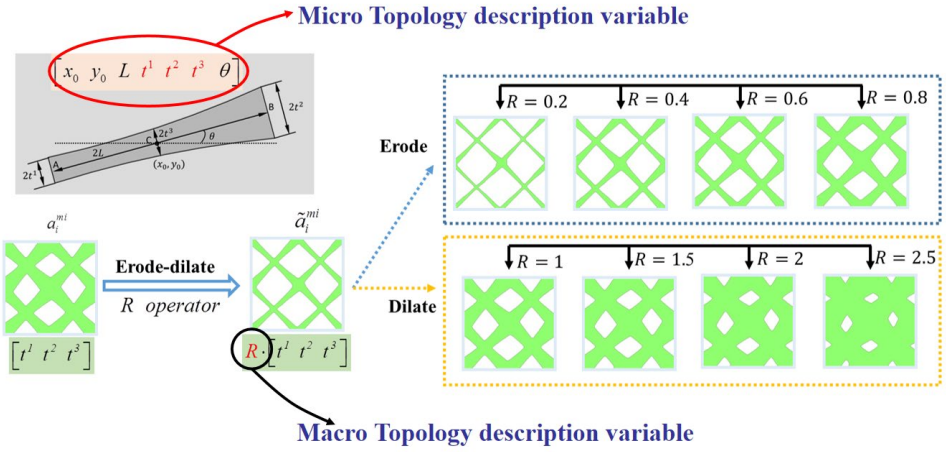

Figure 3. Illustration of the two types of design variables.

In conclusion, two types of design variables are introduced in this paper for describe the topology of a quasi-periodic cellular structure. $\mathbf{D}^{mi}$ is used to optimized the topology of the base unit cell (BUC) and $\boldsymbol{\rho}^{ma}$ is used to optimized the distribution of the quasi-periodic microstructures. Here, the superscript *mi* and *ma* represent that the design variable is defined in macro and micro domain, respectively.

It should be noted that, only the TDF shown as Eq. (5) is considered in this paper for the limited space. But for some other TDFs, it is also very easy to choose alterable parameters.

 doi:10.20944/preprints202407.0902.v1

2.3. Optimization Formulation

In this paper, the optimization of minimum structural compliance with volume constraint is considered, wherein the mathematical formulation can be given as:

$$\begin{aligned} &\text{find} && \boldsymbol{\rho}^{ma},\ \mathbf{D}^{\mathrm{mi}} \\ &\min && c=\mathbf{F}^{\mathrm{T}}\mathbf{U}=\mathbf{U}^{\mathrm{T}}\mathbf{K}\mathbf{U} \\ &\text{s.t.} && \mathbf{K}(\boldsymbol{\rho}^{ma},\mathbf{D}^{\mathrm{mi}})\mathbf{U}=\mathbf{F} \\ & && \int_{D^{mi}} H\left(\phi^{s}\left(\mathbf{x}\right)\right)dV-\overline{V}^{mi}=0 \\ & && \sum_{e=1}^{N^{ma}}\rho_{e}^{ma}v_{e}^{ma}-\overline{V}^{ma}\le 0 \\ & && 0\le\rho_{e}^{ma}\le 1,\ (e=1,\ldots,N^{ma}) \\ & && \mathbf{D}^{mi}\in\Xi_{\mathbf{D}} \end{aligned} \tag{10}$$

where $\boldsymbol{\rho}^{ma}=\left(\rho_{1}^{ma},...,\rho_{e}^{ma},...,\rho_{N^{ma}}^{ma}\right)^{\mathrm{T}}$ and $\mathbf{D}^{mi}=\left(\left(\mathbf{D}^{1}\right)^{\mathrm{T}},...,\left(\mathbf{D}^{i}\right)^{\mathrm{T}},...\left(\mathbf{D}^{N^{mi}}\right)^{\mathrm{T}}\right)^{\mathrm{T}}$ are design variables, N^{ma} represents the number of elements within the macro design domain. H=H(x) is the Heaviside function. $\overline{V}^{mi}$ and $\overline{V}^{ma}$ are the upper bounds of the volume fractions of solid materials in micro and macro scales, respectively. $\overline{V}^{ma}$ is the total material can be used in the design domain and $\overline{V}^{mi}$ is the material used for describe the topology of the BUC. Generally, $\overline{V}^{mi}$ should not be too large and $\overline{V}^{mi}$=0.2 is used in this paper. Large numerical examples show that this can give an stable convergence for most examples. The symbol $\Xi_{\mathbf{D}}$ is the admissible set that $\mathbf{D}^{mi}$ belongs to, and it is usually determined by the upper and lower bounds of the components in each $\mathbf{D}^{i}$, i=1,…,N^{mi}. c is the objective function representing the structural compliance that can be written in the element form as:

$$c=\mathbf{U}^{T}\mathbf{K}\mathbf{U}=\sum_{e=1}^{N^{ma}}\mathbf{U}_{e}^{T}\mathbf{K}_{e}\mathbf{U}_{e} \tag{11}$$

where $\mathbf{K}$, $\mathbf{U}$ and $\mathbf{F}$ are the global stiffness matrix, the displacement vector and the external load vector, respectively. $\mathbf{U}_{e}$ denotes the element displacement vector and $\mathbf{K}_{e}$ is the element stiffness matrix which can be expressed as:

$$\mathbf{K}_{e}=\int_{\Omega_{e}}\mathbf{B}^{T}\mathbf{D}_{e}^{ma}\mathbf{B}d\Omega \tag{12}$$

where Ω_{e} denotes the element domain, $\mathbf{B}$ is the strain-displacement matrix, and $\mathbf{D}_{e}^{ma}\left(\rho_{e}^{ma},\mathbf{D}^{\mathrm{mi}}\right)$ is the elastic matrix of element e in macro-domain.

3. Numerical Implementations

In this section, for using the gradient based optimization method to solve the above optimization formulation. The interpolation schemes between the material properties and the design variables are given firstly. Then the sensitivity analysis of the objective function with respect to (w.r.t.) the two types of design variables are derived.

3.1. Interpolation Scheme

In this paper, the equivalent material elastic matrices of microstructures are computed by asymptotic homogenization (AH) method [48]:

 doi:10.20944/preprints202407.0902.v1

$$\mathbf{D}^{\mathrm{H}}=\frac{1}{|Y|}\int_{Y}\left[\mathbf{D}(\mathbf{y})-\mathbf{D}(\mathbf{y})\varepsilon_{y}(\phi,\mathbf{y})\right]d\mathbf{y} \tag{13}$$

where $\mathbf{y}$ denotes the position coordinate in local coordinate system and $\mathbf{D}(\mathbf{y})$ is the elastic matrix in $\mathbf{y}$ location. As in most topology optimization approaches, structured four node bi-linear elements are used to discretize the design domain uniformly. Since the boundaries of the components can be described accurately and explicitly in the MMC solution framework, finite element method (FEM) analysis with high accuracy can be achieved by resorting to the X-FEM approaches or body-fitted adaptive mesh techniques. In the present work, however, in order to enhance the computational efficiency, the ersatz material model is adopted for FEM analysis. With use of the ersatz material model, once the values of TDF at four nodes of a element are known, the Young's modulus of this element can be interpolated as

$$E^{e}=\frac{E\left(\sum_{i=1}^{4}\left(H\left(\phi_{i}^{e}\right)\right)^{q}\right)}{4} \tag{14}$$

according to (8). In (9), $H=H(x)$ is the Heaviside function and $\phi_{i}^{e},i=1,...,4$ are the values of the TDF function of the whole structure (i.e., $\phi_S(x)$) at four nodes of element e. For numerical implementation purpose, as a common practice in the literature, H(x) is often replaced by its regularized version $H_\epsilon(x)$. In the present work, the form of $H_\epsilon(x)$ is taken as

$$H_{\varepsilon}(x)=\begin{cases}1 & x\\ \dfrac{3(1-\alpha)}{4}\left(\dfrac{x}{\varepsilon}-\dfrac{x^{3}}{3\varepsilon^{3}}\right)+\dfrac{(1+\alpha)}{2} & \\ \alpha & \end{cases} \tag{15}$$

where ε is a parameter that controls magnitude of regularization and α is a small positive number to ensure the nonsingular of the global stiffness matrix. In addition, in the present study, we take q=2. For the ith element, the modified SIMP (Solid Isotropic Material with Penalty) method [49] is applied to interpolate $\mathbf{D}_i$ and $\bar{\tilde{\rho}}_{i}^{mi}$:

$$\mathbf{D}_{i}=\left(\underline{\rho}+(\bar{\rho}-\underline{\rho})\left(\bar{\tilde{\rho}}_{i}^{mi}\right)^{p}\right)\mathbf{D}_{0} \tag{16}$$

where $\mathbf{D}_0$ is the elastic material matrix of the base solid material, subscript i represents the ith element in unit cell. $\underline{\rho}$=0.001 is the lower bound to avoid a singular matrix, $\bar{\rho}$=1 is the upper bound. The power, $p>1$ which is termed the penalization power, is introduced to yield distinctive "0–1" designs. $\varepsilon_{y}(\cdot)$ represents the strain calculator. $\phi=\left[\phi^{11},\phi^{22},\phi^{12}\right]$ denotes the characteristic displacements matrix which is obtained by solving the following equation with periodic boundary conditions:

$$\int_{Y}\varepsilon_{y}^{\mathrm{T}}(\mathbf{v})\left[\mathbf{D}(\mathbf{y})-\mathbf{D}(\mathbf{y})\varepsilon_{y}(\phi)\right]d\mathbf{y}=0,\forall\phi\in V_{y} \tag{17}$$

where $V_{y}=\left\{u_{y}(\mathbf{y})\,|\,\mathbf{y}\in Y,u_{y}(\mathbf{y}+Y)=u_{y}(\mathbf{y})\right\}$ denotes the function space of periodic functions defined in unit cell Y and $\mathbf{v}$ represents the virtual displacement field.

Limited by the computational cost, it is difficult to calculate the effective elastic matrices $\mathbf{D}^{\mathrm{H}}$ of all microstructures obtained by the erode-dilate process, so only some samples are chosen to compute the $\mathbf{D}^{\mathrm{H}}$ and then cubic B-spline is used as the base function to obtain an explicit formulation by least square method:

Preprints.org (www.preprints.org) | NOT PEER-REVIEWED | Posted: 11 July 2024 doi:10.20944/preprints202407.0902.v1

$$\mathbf{D}^{\mathrm{H}}\left(\rho_e^{ma},\rho_i^{mi}\right)=f_{spline}\left(\rho_e^{ma},\rho_i^{mi}\right) \tag{18}$$

denotes the fitting curves of D_{11}, D_{12}, D_{22} and D_{33} with the variation of ρ_e^{ma} in example 1. The red points are the samples points and the black lines are the fitting curves. $f_{spline}\left(\rho_e^{ma},\rho_i^{mi}\right)$ is an explicit function whose values and derivative with ρ_e^{ma} can be computed very easily.

For avoiding the microstructures with small volume fraction, which are difficult for manufacture, appear in the optimized results, a penalization scheme is applied:

$$\mathbf{D}_e^{ma}\left(\rho_e^{ma},\rho_i^{mi}\right)=\left(\rho_e^{ma}\right)^q f_{spline}\left(\rho_e^{ma},\rho_i^{mi}\right) \tag{19}$$

where q is the penalization power. The following values of q are suggested:

$$q=\begin{cases}3 & \rho_e^{ma}<0.1\\ 0 & \rho_e^{ma}\geq 0.1\end{cases} \tag{20}$$

3.2. Sensitivity Analysis

In order to use the gradient-based optimization method, the sensitivities of the objective function with respect to (w.r.t.) the design variables are derived in this section. Since the sensitivities of the volume constraint functions w.r.t. the design variables are trivial and therefore are not given in this paper. The sensitivity of the structural compliance w.r.t x_j $(=\rho_i^{mi},\rho_e^{ma})$ can be obtained based on adjoint method:

$$\frac{\partial c}{\partial x_j}=-\sum_e^{N^{ma}}\mathbf{U}_e^T\left(\int_{\Omega_e}\mathbf{B}^T\frac{\partial\mathbf{D}_e^{ma}}{\partial x_j}\mathbf{B}dV\right)\mathbf{U}_e \tag{21}$$

Note that, for different design variables (ρ_i^{mi},ρ_e^{ma}), the main difference is the derivation of elastic matrix $\mathbf{D}_e^{ma}$ to the design variables. Therefore, the sensitivities of the objective function with respect to ρ_e^{ma} and ρ_i^{mi} will be given respectively.

(1) Sensitivities w.r.t. ρ_e^{ma}

Differentiating Eq. to ρ_e^{ma} yields:

$$\frac{\partial\mathbf{D}_e^{ma}}{\partial\rho_j^{ma}}=\begin{cases}0 & e=j\\ q\left(\rho_j^{ma}\right)^{q-1}f_{spline}\left(\rho_e^{ma},\rho_i^{mi}\right) & \\ +\left(\rho_j^{ma}\right)^q\dfrac{\partial f_{spline}\left(\rho_e^{ma},\rho_i^{mi}\right)}{\partial\rho_j^{ma}} & e\neq j\end{cases} \tag{22}$$

Then, substituting it into Eq., the sensitivity of the structural compliance with respect to ρ_e^{ma} can be written as:

$$\begin{aligned}\frac{\partial c}{\partial\rho_e^{ma}}=&-p\left(\rho_e^{ma}\right)^{p-1}\mathbf{U}_e^{\mathrm{T}}\left(\int_{\Omega_e}\mathbf{B}^{\mathrm{T}}f_{spline}\left(\rho_e^{ma},\rho_i^{mi}\right)\mathbf{B}dV\right)\mathbf{U}_e\\ &-\left(\rho_e^{ma}\right)^p\mathbf{U}_e^{\mathrm{T}}\left(\int_{\Omega_e}\mathbf{B}^{\mathrm{T}}\frac{\partial f_{spline}\left(\rho_e^{ma},\rho_i^{mi}\right)}{\partial\rho_e^{ma}}\mathbf{B}dV\right)\mathbf{U}_e\end{aligned} \tag{23}$$

 doi:10.20944/preprints202407.0902.v1

where subscript $e = 1, 2, ..., N_{ma}$.

(2) Sensitivities w.r.t. D_i^{mi}

According to Eq., the sensitivity of the objective function w.r.t ρ_i^{mi} can be written as:

$$\frac{\partial c}{\partial D_i^{mi}} = \frac{\partial c}{\partial \rho_j^{mi}} \cdot \frac{\partial \rho_j^{mi}}{\partial D_i^{mi}} = -\sum_{r=1}^{N^{ma}} u_r^T \cdot (\mathrm{f}(\rho_r^{ma}) \cdot \int_{\Omega_e} B^T \frac{\partial D_r(\rho_j^{mi}, \rho_e^{ma})}{\partial \rho_j^{mi}} \cdot \frac{\partial \rho_j^{mi}}{\partial D_i^{mi}} B \cdot d\Omega_e) \cdot u_r \tag{24}$$

Note that $\partial c / \partial \rho_i^{mi}$ is a summation of the elements in the macro-domain:

$$\frac{\partial \rho_j^{mi}}{\partial D_i^{mi}} = \sum_{k=1}^{4} (q \cdot H(\phi_k^j)^{q-1} \cdot \frac{\partial H(\phi_k^j)}{\partial D_i^{mi}}) / 4 \tag{25}$$

4. Numerical Examples

In this section, the proposed method is applied to the design of layer-wised beam problem, cantilever beam problem and MBB problem. The detail descriptions of the examples will be given in the subsections, respectively. For all examples, fixed mesh of 4-node bilinear square elements is used to discrete the macro design domain and micro design domain. Unless otherwise noted, the micro-design domain is discretized by 50*50 square elements. The material is isotropic with Young's modulus *E*=206 MPa and Poisson's ratio $\mu = 0.28$. Initial values of the design variables ρ_e^{ma} and ρ_i^{mi} are set to be equal to the volume fractions $\overline{V}^{ma}$ and $\overline{V}^{mi}$, respectively. It should be noted that, the volume fraction of the base unit cell $\overline{V}^{mi}$ is chosen as 0.2 in this paper. For the design variables ρ_e^{ma} defined in macro-domain, the density filtering technique with filtering radius $r^{ma} = 1.5$ is applied to avoid the check-board phenomena. All the optimization problems are solved using the gradient driven MMA algorithm. The convergence criterion is chosen as: $\max \left\| x^{i+1} - x^i \right\| \le 1e-3$ and the maximum iteration number is 300.

4.1. Short Cantilever Beam Problem

As the first test case, the problem of minimum compliance for a cantilever beam is considered. The design domain (shown in Figure 4) is a rectangle of dimension 20 by 15 and the left side of the domain is fixed. 20*15 square elements are used to discretize the it and a vertical point load *F*=1*KN* at the right bottom corner is added. The volume fractions of the total material chosen as 0.4.

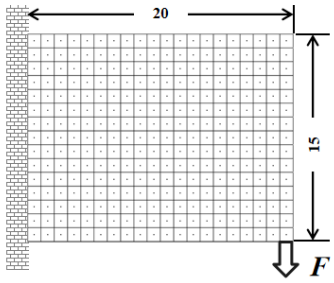

Figure 4. Illustration of the design model.

Preprints.org (www.preprints.org) | NOT PEER-REVIEWED | Posted: 11 July 2024 doi:10.20944/preprints202407.0902.v1

(a) Microstructural topology **(b) Macrostructural layout** **(c) Quasi-periodic cellular**

Figure 5. The final optimized structure obtained by the proposed method: *c*=21.73.

The final optimized quasi-periodic cellular structure is shown in Figure 5, whose compliance is 27.73.Classical single-scale SIMP method [50] and periodic cellular structural topology optimization [23] are also used to solve this problem, and the results are shown in Figure 6(a) and (b), respectively. Here, the volume fraction of the periodic microstructure is set as 0.6. The structural compliances of these two results are 27.85 and 52.81, respectively. They are all larger than the compliance of the result obtained by the proposed method.

Figure 6. The optimized results: a) single-scale structure: c=27.85, b) uniform microstructure: c=52.81.

4.2. Long Cantilever Beam Problem

As the second test case, the problem of minimum compliance for a cantilever beam is considered. The design domain (shown in Figure 7) is a rectangle of dimension 120 by 30 and the left side of the domain is fixed. 120*30 square elements are used to discretize the it and a vertical point load F=1KN at the right bottom corner is added. The volume fractions of the total material chosen as 0.4.

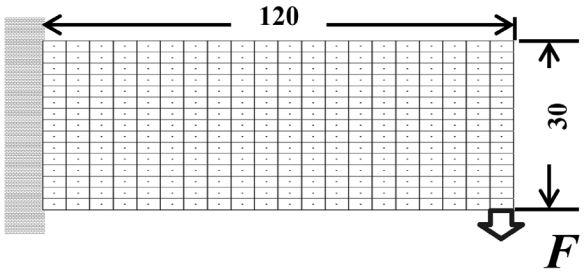

Figure 7. Illustration of the design model.

Figure 8 denotes the iteration process of the proposed method, including the topology of the base unit cell and density distribution in the macro domain. The slight oscillations in the iteration curve are caused by the changes of parameters. The final optimized quasi-periodic cellular structure is shown in Figure 9, whose compliance is 269.73.

Preprints.org (www.preprints.org) | NOT PEER-REVIEWED | Posted: 11 July 2024 doi:10.20944/preprints202407.0902.v1

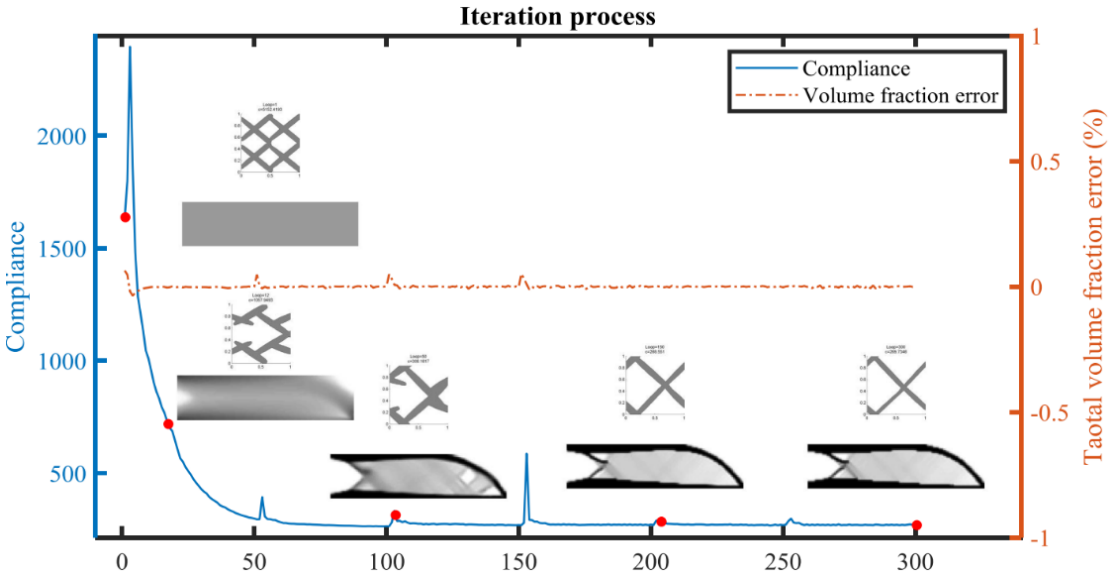

Figure 8. Iteration process.

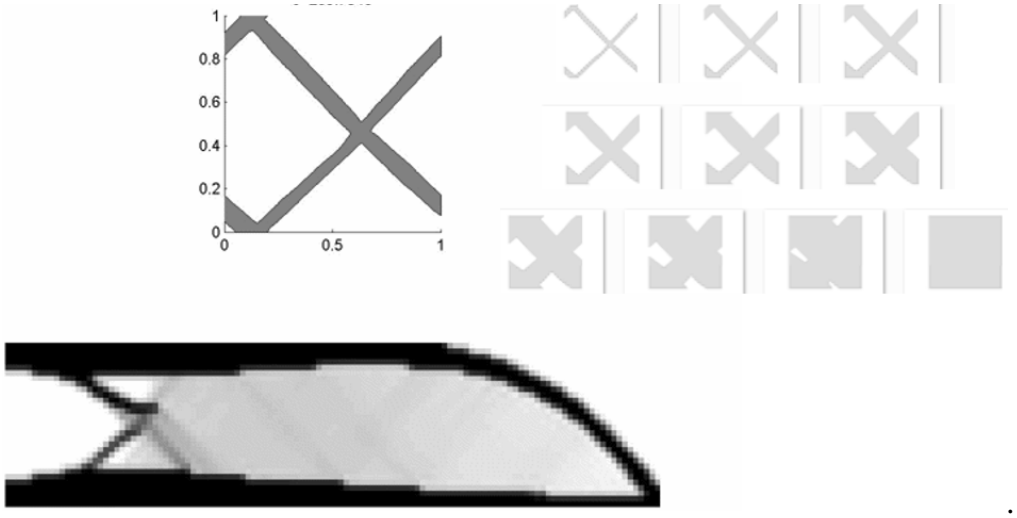

Figure 9. The final optimized structure obtained by the proposed method: *c=269.73.*

5. Conclusions

This paper proposes a new topology optimization method for the design of quasi-periodic cellular structures using a hybrid MMC-density approach. The quasi-periodic microstructures are described by MMC method with different thickness of bars. Then the microstructural topology of the base unit cell and the distribution the quasi-microstructures are optimized simultaneously. Interpolation functions between element elastic matrix and the two types of design variables are established and the sensitives of the objective function with respect to the two types of the design variables can be derived for using the gradient-based optimization method to solve the optimization model. Numerical examples show that the quasi-periodic structures have a great performance improvement compared to the periodic structures, while only finite extra computational cost is needed. The added computational cost is caused by computing the equivalent material elastic matrices of the quasi-microstructures. Furthermore, even for the minimum compliance problem, the quasi-periodic structures have lower objectives than solid structures, which is difficult to be achieved by periodic structures.

Acknowledgments: This work is financially supported by the National Natural Science Foundation of China (Grant Nos. 52375253 and 12202154) and Dreams Foundation of Jianghuai Advance Technology Center (NO.20240102).

References

1. Duncan, O.; Shepherd, T.; Moroney, C.; Foster, L.; Venkatraman, D. P.; Winwood, K.; Allen, T.; Alderson, A. Review of Auxetic Materials for Sports Applications: Expanding Options in Comfort and Protection. *Applied Sciences* **2018**, *8*.
2. Xiao, Z.; Yang, Y.; Xiao, R.; Bai, Y.; Song, C.; Wang, D. Evaluation of topology-optimized lattice structures manufactured via selective laser melting. *Materials & Design* **2018**, *143*, 27-37.
3. Tang, Y.; Dong, G.; Zhou, Q.; Zhao, Y. F. Lattice Structure Design and Optimization With Additive Manufacturing Constraints. *IEEE Transactions on Automation Science and Engineering* **2018**, *15*, 1546-1562.
4. Panesar, A.; Abdi, M.; Hickman, D.; Ashcroft, I. Strategies for functionally graded lattice structures derived using topology optimisation for Additive Manufacturing. *Additive Manufacturing* **2018**, *19*, 81-94.
5. Zhu, J.-H.; Zhang, W.-H.; Xia, L. Topology optimization in aircraft and aerospace structures design. *Archives of Computational Methods in Engineering* **2015**, 1-28.
6. Liu, S.; Hu, R.; Li, Q.; Zhou, P.; Dong, Z.; Kang, R. Topology optimization-based lightweight primary mirror design of a large-aperture space telescope. *Applied Optics* **2014**, *53*, 8318-8325.
7. Clausen, A.; Wang, F.; Jensen, J. S.; Sigmund, O.; Lewis, J. A. Topology Optimized Architectures with Programmable Poisson's Ratio over Large Deformations. *Advanced Materials* **2015**, *27*, 5523-5527.
8. Huang, X.; Zhou, S.; Sun, G.; Li, G.; Xie, Y. M. Topology optimization for microstructures of viscoelastic composite materials. *Computer Methods in Applied Mechanics and Engineering* **2015**, *283*, 503-516.
9. Osanov, M.; Guest, J. K. Topology Optimization for Architected Materials Design. *Annual Review of Materials Research* **2016**, *46*, 211-233.
10. Chen, W.; Liu, S. Topology optimization of microstructures of viscoelastic damping materials for a prescribed shear modulus. *Structural and Multidisciplinary Optimization* **2014**, *50*, 287-296.
11. Guo, X.; Cheng, G.-D. Recent development in structural design and optimization. *Acta Mechanica Sinica* **2010**, *26*, 807-823.
12. Sigmund, O.; Maute, K. Topology optimization approaches. *Structural and Multidisciplinary Optimization* **2013**, *48*, 1031-1055.
13. van Dijk, N. P.; Maute, K.; Langelaar, M.; van Keulen, F. Level-set methods for structural topology optimization: a review. *Structural and Multidisciplinary Optimization* **2013**, *48*, 437-472.
14. Xia, L.; Xia, Q.; Huang, X.; Xie, Y. M. Bi-directional Evolutionary Structural Optimization on Advanced Structures and Materials: A Comprehensive Review. *Archives of Computational Methods in Engineering* **2016**.
15. Aage, N.; Andreassen, E.; Lazarov, B. S.; Sigmund, O. Giga-voxel computational morphogenesis for structural design. *Nature* **2017**, *550*, 84-86.
16. Liu, H.; Wang, Y.; Zong, H.; Wang, M. Y. Efficient structure topology optimization by using the multiscale finite element method. *Structural and Multidisciplinary Optimization* **2018**, *58*, 1411-1430.
17. Sigmund, O. Materials with prescribed constitutive parameters: An inverse homogenization problem. *International Journal of Solids and Structures* **1994**, *31*, 2313-2329.
18. Groen, J. P.; Sigmund, O. Homogenization-based topology optimization for high-resolution manufacturable microstructures. *International Journal for Numerical Methods in Engineering* **2018**, *113*, 1148-1163.
19. Rodrigues, H.; Guedes, J. M.; Bendsoe, M. P. Hierarchical optimization of material and structure. *Structural and Multidisciplinary Optimization* **2002**, *24*, 1-10.
20. Xia, L.; Breitkopf, P. Concurrent topology optimization design of material and structure within FE2 nonlinear multiscale analysis framework. *Computer Methods in Applied Mechanics and Engineering* **2014**, *278*, 524-542.
21. Xia, L.; Breitkopf, P. Multiscale structural topology optimization with an approximate constitutive model for local material microstructure. *Computer Methods in Applied Mechanics and Engineering* **2015**, *286*, 147-167.
22. Coelho, P. G.; Rodrigues, H. C. Hierarchical topology optimization addressing material design constraints and application to sandwich-type structures. *Structural and Multidisciplinary Optimization* **2015**, *52*, 91-104.
23. Liu, L.; Yan, J.; Cheng, G. Optimum structure with homogeneous optimum truss-like material. *Computers & Structures* **2008**, *86*, 1417-1425.
24. Yan, J.; Cheng, G.-d.; Liu, L. A uniform optimum material based model for concurrent optimization of thermoelastic structures and materials. *International Journal for Simulation and Multidisciplinary Design Optimization* **2008**, *2*, 259-266.
25. Long, K.; Han, D.; Gu, X. Concurrent topology optimization of composite macrostructure and microstructure constructed by constituent phases of distinct Poisson's ratios for maximum frequency. *Computational Materials Science* **2017**, *129*, 194-201.

 doi:10.20944/preprints202407.0902.v1

26. Yan, J.; Guo, X.; Cheng, G. Multi-scale concurrent material and structural design under mechanical and thermal loads. *Computational Mechanics* **2016**, *57*, 437-446.
27. Long, K.; Wang, X.; Gu, X. Concurrent topology optimization for minimization of total mass considering load-carrying capabilities and thermal insulation simultaneously. *Acta Mechanica Sinica* **2017**.
28. Xu, B.; Huang, X.; Xie, Y. M. Two-scale dynamic optimal design of composite structures in the time domain using equivalent static loads. *Composite Structures* **2016**, *142*, 335-345.
29. Andreassen, E.; Jensen, J. S. Topology optimization of periodic microstructures for enhanced dynamic properties of viscoelastic composite materials. *Structural and Multidisciplinary Optimization* **2014**, *49*, 695-705.
30. Du, J.; Yang, R. Vibro-acoustic design of plate using bi-material microstructural topology optimization. *Journal of Mechanical Science and Technology* **2015**, *29*, 1413-1419.
31. Zheng, J.; Luo, Z.; Li, H.; Jiang, C. Robust topology optimization for cellular composites with hybrid uncertainties. *International Journal for Numerical Methods in Engineering* **2018**, *115*, 695-713.
32. Zheng, J.; Luo, Z.; Jiang, C.; Gao, J. Robust topology optimization for concurrent design of dynamic structures under hybrid uncertainties. *Mechanical Systems and Signal Processing* **2019**, *120*, 540-559.
33. Deng, J.; Yan, J.; Cheng, G. Multi-objective concurrent topology optimization of thermoelastic structures composed of homogeneous porous material. *Structural and Multidisciplinary Optimization* **2013**, *47*, 583-597.
34. Zhang, P.; Toman, J.; Yu, Y.; Biyikli, E.; Kirca, M.; Chmielus, M.; To, A. C. Efficient Design-Optimization of Variable-Density Hexagonal Cellular Structure by Additive Manufacturing: Theory and Validation. *Journal of Manufacturing Science & Engineering* **2015**, *137*.
35. Wang, X.; Zhang, P.; Ludwick, S.; Belski, E.; To, A. C. Natural frequency optimization of 3D printed variable-density honeycomb structure via a homogenization-based approach. *Additive Manufacturing* **2017**.
36. Cheng, L.; Bai, J.; To, A. C. Functionally graded lattice structure topology optimization for the design of additive manufactured components with stress constraints. *Computer Methods in Applied Mechanics and Engineering* **2019**, *344*, 334-359.
37. Wu, Z.; Xia, L.; Wang, S.; Shi, T. Topology optimization of hierarchical lattice structures with substructuring. *Computer Methods in Applied Mechanics and Engineering* **2019**, *345*, 602-617.
38. Wang, Y.; Chen, F.; Wang, M. Y. Concurrent design with connectable graded microstructures. *Computer Methods in Applied Mechanics and Engineering* **2017**, *317*, 84-101.
39. Wang, Y.; Zhang, L.; Daynes, S.; Zhang, H.; Feih, S.; Wang, M. Y. Design of graded lattice structure with optimized mesostructures for additive manufacturing. *Materials & Design* **2018**, *142*, 114-123.
40. Zong, H.; Liu, H.; Ma, Q.; Tian, Y.; Zhou, M.; Wang, M. Y. VCUT level set method for topology optimization of functionally graded cellular structures. *Computer Methods in Applied Mechanics and Engineering* **2019**, *354*, 487-505.
41. Guo, X.; Zhang, W.; Zhong, W. Doing Topology Optimization Explicitly and Geometrically—A New Moving Morphable Components Based Framework. *Journal of Applied Mechanics* **2014**, *81*, 081009-081009-081012.
42. Guo, X.; Zhang, W.; Zhang, J.; Yuan, J. Explicit structural topology optimization based on moving morphable components (MMC) with curved skeletons. *Computer Methods in Applied Mechanics and Engineering* **2016**, *310*, 711-748.
43. Zhang, W.; Chen, J.; Zhu, X.; Zhou, J.; Xue, D.; Lei, X.; Guo, X. Explicit three dimensional topology optimization via Moving Morphable Void (MMV) approach. *Computer Methods in Applied Mechanics and Engineering* **2017**, *322*, 590-614.
44. Svanberg, K. The method of moving asymptotes—a new method for structural optimization. *International journal for numerical methods in engineering* **1987**, *24*, 359-373.
45. Zhang, W.; Zhao, L.; Gao, T.; Cai, S. Topology optimization with closed B-splines and Boolean operations. *Computer Methods in Applied Mechanics and Engineering* **2017**, *315*, 652-670.
46. Zhang, W.; Zhou, Y.; Zhu, J. A comprehensive study of feature definitions with solids and voids for topology optimization. *Computer Methods in Applied Mechanics and Engineering* **2017**, *325*, 289-313.
47. Zhang, W.; Yuan, J.; Zhang, J.; Guo, X. A new topology optimization approach based on Moving Morphable Components (MMC) and the ersatz material model. *Structural and Multidisciplinary Optimization* **2016**, *53*, 1243-1260.
48. Papanicolau, G.; Bensoussan, A.; Lions, J.-L.: *Asymptotic analysis for periodic structures*; Elsevier, 1978.
49. Bendsøe, M. P.; Sigmund, O. Material interpolation schemes in topology optimization. *Archive of applied mechanics* **1999**, *69*, 635-654.
50. Bendsøe, M. P.; Sigmund, O. Material interpolation schemes in topology optimization. *Archive of Applied Mechanics* **1999**, *69*, 635-654.

 doi:10.20944/preprints202407.0902.v1

disclaim responsibility for any injury to people or property resulting from any ideas, methods, instructions or products referred to in the content.